Journal of Theoretical and Applied Information Technology
10th March 2014. Vol. 61 No.1

ISSN: 1992-8645 www.jatit.org E-ISSN: 1817-3195

MRI BRAIN SEGMENTATION VIA HYBRID FIREFLY SEARCH ALGORITHM

[1]WALEED ALOMOUSH, [2]SITI NORUL HUDA SHEIKH ABDULLAH, [3]SHAHNORBANUN SAHRAN, [4]RIZUANA IQBAL HUSSAIN

[123]Pattern Recognition Research Group, Center for Artificial Intelligence Technology ,Faculty of Information Science and Technology,Universiti Kebangsaan Malaysia, 43600, Bangi, Selangor D.E., Malaysia.

Department of Radiology Universiti Kebangsaan Malaysia Medical Centre, 56000 Cheras, Kuala Lumpur, Malaysia.

Email: [1]waleedomoush2000@yahoo.com , [2]mimi@ftsm.ukm.my , [3]shah@ftsm.ukm.my , [4]rizuana@ppukm.ukm.my

ABSTRACT

Magnetic resonance imaging (MRI) brain tumor segmentation is a challenging tasks which include the detection task of tumor from images. In general, this process is done manually by experts in medical images field which is always unclear, because the similarity between normal and abnormal tissues. The present study proposes a new clustering approach based on the hybridization of firefly algorithm (FA) and fuzzy c-means algorithm(FCM) called (FFCM) to segment MRI brain images. this approach use the capability of firefly search to find optimal initial cluster centres for the FCM and thus improve (MRI) brain tumor segmentation. The proposed approach was evaluated by applying it to a magnetic resonance imaging (MRI) brain segmentation problem using a simulated brain data set of McGill University and real MRI images from Internet Brain Segmentation Repository benchmark data sets. The cluster validity index (Rm) was used as a fitness function to determine the best solutions obtained by the firefly algorithm. The experiments indicated encouraging results after applying FFCM, compared with the outcomes of state-of-the-art segmentation algorithms and FCM random initialization of cluster centres.

Keywords: *Fuzzy c-means, Firefly algorithm, MRI Images segmentation, Rm validity index*

1. INTRODUCTION

The process of digital image analysis comprises a lot of steps or phases, and image segmentation is one of the most significant and intricate. In this phase, images are segmented into many components and each component contains some identical attributes [1] . Image segmentation considered a basic role in many different domains. In medical imaging for instance, Magnetic resonance imaging (MRI) images segmentation techniques can assist doctors and radiologists locate tumors and other pathologies, diagnose illnesses, therapy evaluation, aid in computer guided surgery, measure tissue volume, treatment planning, study anatomical structure, and also surgical simulation [2].

Moreover, different sequences of MRI images are available from these imaging modalities such as T1-Weighted Image (T1WI), Short Tau Inversion Recovery (STIR), T2-Weighted Image (T2WI), Fluid Attenuation Inversion Recovery (FLAIR), etc., where each sequence provides different types of information for the tissues under study. Furthermore, there is the issue of image complexity, which pertains to the amount of subjective information contained in images. Thus, many methods was proposed over the last decades, each of which uses different induction principles [2-3]. These algorithms can be categorized into various groups such as thresholding-based, deformable models-based, clustering-based, histograms-based, classification-based, etc.[2-3]. Fuzzy clustering technique, one of the most frequently methods used in images segmentation due to the most images has unclear boundaries between their segments. As well as, fuzzy clustering algorithms has capability to solve unclear boundaries problem between image regions. It is therefore possible that the fuzzy clustering techniques such as the fuzzy c-means (FCM) algorithm[4], is the most frequently methods used in images

ISSN: 1992-8645 www.jatit.org E-ISSN: 1817-3195

segmentation[5-6]. Both image segmentation and clustering share the same goal of finding accurate classification of their input. The image pixels in clustering methods represented as patterns and each pixel is belong to a cluster (image segment) based on similarity and distance[7].

Over the last few decades, many algorithms for metaheuristic search have been applied in conjunction with the FCM algorithm to find optimal cluster centres. These algorithms explore the entire search space in the problem to determine possible solutions[8]. These algorithms include bee optimization[9], harmony search[10], the ant colony algorithm[11], simulated annealing[12], the genetic algorithm[13-14], tabu search[15], the firefly algorithm[16] and particle swarm[17]. However, to the best of the authors' knowledge, this present study is the first time that a firefly fuzzy c-means (FFCM) algorithm has been applied to image segmentation. Specifically, the present study explores the addition of a firefly algorithm (FA) to FCM to solve the brain MRI image segmentation problem because this is a very complicated domain due to the natural difficulties inherent in MRI image segmentation.

The present study explores the efficiency of the FA in generating near-optimal initial cluster centres for the FCM algorithm, in order to ensure that superior and constant MRI image segmentation outcomes are generated. The FA is one of the more recent algorithms, and as the name implies, is inspired by the behaviour of fireflies[18]. It is worth mentioning that the FA has been employed to resolve nonlinear optimization problems. Generally, in social insect colonies, such as a firefly colony, even though every single individual appears to have an individual routine, the group as a whole seems to be extremely structured. Basically, algorithms that are based on nature have been proved to be effective and efficient in resolving challenging optimization problems. A swarm is a collection of multi-agent systems, such as fireflies, in which the basic agents synchronize their routines to resolve the complicated issue of assigning communication to numerous forage sites in changing circumstances. The remainder of the paper is structured as follows: section 2 provides an overview of the firefly search algorithm; section 3 describes fuzzy clustering with FCM; section 4 discusses the proposed method; section 5 details the results of experiments applying the FFCM algorithm and compares them with other methods; and finally, section 6 presents the conclusion.

2. FIREFLY SEARCH ALGORITHM

Fireflies are among the rarest insects on the planet and have a natural capacity to illuminate themselves in the dark with flickering and glowing biological lights. The FA was motivated by the biological behaviour of fireflies[18]; generally, the FA employs the following three rules: (1) fireflies are unisexual, therefore every individual firefly will be fascinated by another firefly, irrespective of its gender; (2) the unique feature of the glowing light of fireflies will attract prey; and (3) the attraction of fireflies is proportionate to their brightness, which makes the less bright firefly move towards a more brightly glowing firefly .

The population-based FA is capable of discovering the global optima of objective functions, depending on the intelligence of the swarm[19]. Moreover, the FA also examines the foraging behaviour of fireflies. In the FA, the physical entities are arbitrarily spread in the search space, in this case the physical gentility is fireflies, which have a substance known as luciferin that makes the fireflies glow in dark, and generally luciferin will discharge light that is proportional to this value. As mentioned earlier, the fireflies with slightly dimmer light will be attracted towards the brighter individuals; nevertheless the degree of attraction will reduce if the distance between those fireflies increases. On the other hand, if any firefly fails to find another firefly that is brighter than itself, then the former will travel arbitrarily. When the FA is employed to solve clustering problems, the cluster centres are the decision variables, and the objective function is associated with the value of all Euclidean distance training set cases in an N-dimensional space[20].

Depending on the intended function, in the beginning all the agents (fireflies) will be arbitrarily spread all over the search space. The following are the two stages of the FA: the first stage involves the difference in the intensity of light, where the intensity of light is associated with the objective values[21]. Therefore in the case of a maximization/minimization problem, a firefly with higher or lower intensity will entice another individual with higher or lower intensity. Let us presume that there is a swarm of n agents

Journal of Theoretical and Applied Information Technology
10th March 2014. Vol. 61 No.1

ISSN: 1992-8645 www.jatit.org E-ISSN: 1817-3195

(fireflies), where x_i signifies the solution of a firefly i, while its fitness value is signified by $f(x_i)$; furthermore, the current position i of its fitness value f(x) is determined by the brightness I of a firefly[21], thus:

$$I_i = f(x_i), \quad 1 \le i \le n . \qquad (1)$$

The second stage involves movements towards attractive fireflies: the attractive force of a firefly is proportionate to the intensity of light witnessed by nearby fireflies[21]. Every single firefly possesses its unique attraction β, which indicates the power of attraction over individuals of the swarm. This attractiveness β will change with the distance r_{ij} between two fireflies i and j at locations x_i and x_j, respectively, as denoted by the following:

$$r_{ij} = \|x_i - x_j\| , \qquad (2)$$

The attractiveness function β(r) of the firefly is established by

$$\beta(r) = \beta_0 e^{-\gamma r^2} , \qquad (3)$$

if β_0 is the attractiveness at $r = 0$, and γ is the coefficient of the ingestion of light. The motion of a firefly i from position x_i, which is attracted to another much more attractive (brighter) firefly j at position x_j is denoted by

Pseudo-code: A High-Level Description of firefly algorithm
Input:
Create an initial population of fireflies n within d-dimensional search space x_{ik}, $i = 1, 2, \ldots, n$ and $k = 1, 2, \ldots, d$
Evaluate the fitness of the population $f(x_{ik})$ which is directly proportional to light intensity I_{ik}
Algorithm's parameter—β_0, γ
Output:
Obtained minimum location: $x_{i\min}$
begin
  repeat
    for $i = 1$ to n
      for $j = 1$ to n
        if ($I_j < I_i$)
          Move firefly i toward j in d-dimension using Eq. (4)
        end if
        Attractiveness varies with distance r via $\exp[-r^2]$
        Evaluate new solutions and update light intensity using Eq. (1)
      end for j
    end for i
    Rank the fireflies and find the current best
  until stop condition true
end

Fig. 1. Firefly Algorithm Pseudo-Code.

$$x_{i\,(t+1)} = x_{i\,(t)} + \beta_0 e^{-\gamma r_{ij}^2}(x_i - x_j) + \propto \left(\text{rand} - \frac{1}{2}\right) \qquad (4)$$

A comprehensive explanation of the FA can be found in[18] and the pseudo-code for this algorithm is given in Fig. 1.

3. CLUSTERING WITH FUZZY C-MEANS

Clustering is a unsupervised learning approach that is capable of partitioning identical data objects (patterns) based on some level of similarity, which increases the similarity of objects within a group and decreases the similarity among objects between various groups[22-23]. A clustering algorithm for grouping fuzzy data is carried out on a collection of n objects (pixels) $\{x_1, x_2, \ldots, x_n\}$, and each of these objects is $x_i \in \Re^d$, a characteristic vector which consists of d real-valued dimensions that reveal the characteristics of the object depicted by x_i . A fuzzy membership matrix, referred to as fuzzy partition $U = [u_{ij}]_{c\times n}$ ($U \in M_{fcn}$ as in Eq. 1). The equation

$$M_{fcn}\left\{ U \in \Re^{c\times n} \;\middle|\; \sum_{j=1}^{c} U_{ij} = 1, 0 < \sum_{i=1}^{n} U_{ij} < n \text{ , and } U_{ij} \in [0,1]; 1 \le j < c, ; 1 < i \le n \right\} \qquad (5)$$

represents the fuzzy clusters c of the objects, where signifies the fuzzy membership of the ith object to the jth fuzzy cluster. For example, each and every data object is related to a specific (probably zero) degree of every single fuzzy cluster. A FCM algorithm is a repetitive technique capable of locally decreasing the following objective functions:

$$J_m = \sum_{i=1}^{c}\sum_{i=1}^{n} u_{ij}^{m} \|x_i - v_j\|^2 , \qquad (6)$$

where $\{v_j\}_{j=1}^{c}$ is the centroids of the clusters c, which indicates the standard of the inner product $\|.\|$ (e.g., Euclidean distance) from the data point x_i to the jth cluster centre; furthermore, the parameter $m \in [1, \infty)$ is a distort proponent on each fuzzy membership, which ascertains the level of fuzziness of the ensuing classification. The following is a summary of the FCM steps and Fig. 2 below illustrates the FCM pseudo-code:

1. Choose the number of fuzzy clusters c.
2. Choose initial cluster centres $v_1, v_2, \ldots, v_c$.

Journal of Theoretical and Applied Information Technology
10th March 2014. Vol. 61 No.1

ISSN: 1992-8645 www.jatit.org E-ISSN: 1817-3195

3. Estimate the components of the fuzzy partition matrix:

$$U_{ij} = \frac{1}{\sum_{k=1}^{c}\left(\frac{\|x_i - v_j\|}{\|x_i - v_k\|}\right)^{\frac{2}{m-1}}} \quad (7)$$

4. Calculate the cluster centres:

$$v_j = \frac{\sum_{i=1}^{n} u_{ij}^{m} \cdot x_i}{\sum_{i=1}^{n} u_{ij}^{m}} \quad (8)$$

5. Repeat steps 3 and 4 until the number of iterations (t) surpasses the set limit, or a termination criterion is met:

$$\|v_{new} - v_{old}\| < \varepsilon \quad (9)$$
where $\varepsilon < 0.001$

The FCM Algorithm
begin
Fix $c, 2 < c < n$;
Fix $\epsilon, (e.g., \epsilon = 0.001)$;
Fix maxIerations, (e.g., maxIerations=100);
Choose any inner product norm metric (e.g., Euclidean distance);
Fix $m, 1 < m < \infty, (e.g., m = 2)$;;
Randomly initialize $v_{0=v1,v2,...,vc}$ cluster centers;
for t = 1 to maxIterations do
Update the membership matrix U using Eq. 7;
Calculate the new cluster centers V^t using Eq. 8;
Calculate the new objective function J_m^t using Eq. 6;
if $(abs(J_m^t - J_m^{t-1} < \epsilon)$ then
break;
else
$J_m^{t-1} = J_m^t$;;
end if
end for
end

Fig.2.FCM Pseudo-Code.

1. Proposed method

In this section we investigate the performance of the FA in terms of obtaining near-optimal cluster centres values in the initialization phase in the FCM algorithm. Here, we propose a clustering approach that consists of two phases (see Fig. 3 below). In the first phase, the FA examines the search space of the given data set to determine the near-optimal cluster centres and then those cluster centres are assessed by making use of the redefined FCM objective function. In the second phase, the finest cluster centres that have been identified are employed as the preliminary cluster centres for the FCM algorithm. The two phases are discussed below.

1.1 Identifying near-optimal cluster centres using firefly search

The cluster centres of the provided data set are encoded by each and every solution of the firefly search. The solution will be as in Eq. 10:

$$= \begin{pmatrix} s_1 & s_2 & s_3 \\ a_1 a_2 \ldots a_d, & a_1 a_2 \ldots a_d, & a_1 a_2 \ldots a_d \end{pmatrix}, \quad (10)$$

where a_i is a numerical characteristic that explains a cluster centre and $a_i \in A$, where A is the collection of the feasible array of each and every pixel attribute. Consequently, each cluster centre s_i is defined by d numerical feature$\{a_1, a_2, \ldots, a_d\}$. As a result, every single solution has an actual size of $(c \times d)$, where c represents a given number of clusters and d indicates the feature number outlining the given data set.

Journal of Theoretical and Applied Information Technology
10th March 2014. Vol. 61 No.1

ISSN: 1992-8645 www.jatit.org E-ISSN: 1817-3195

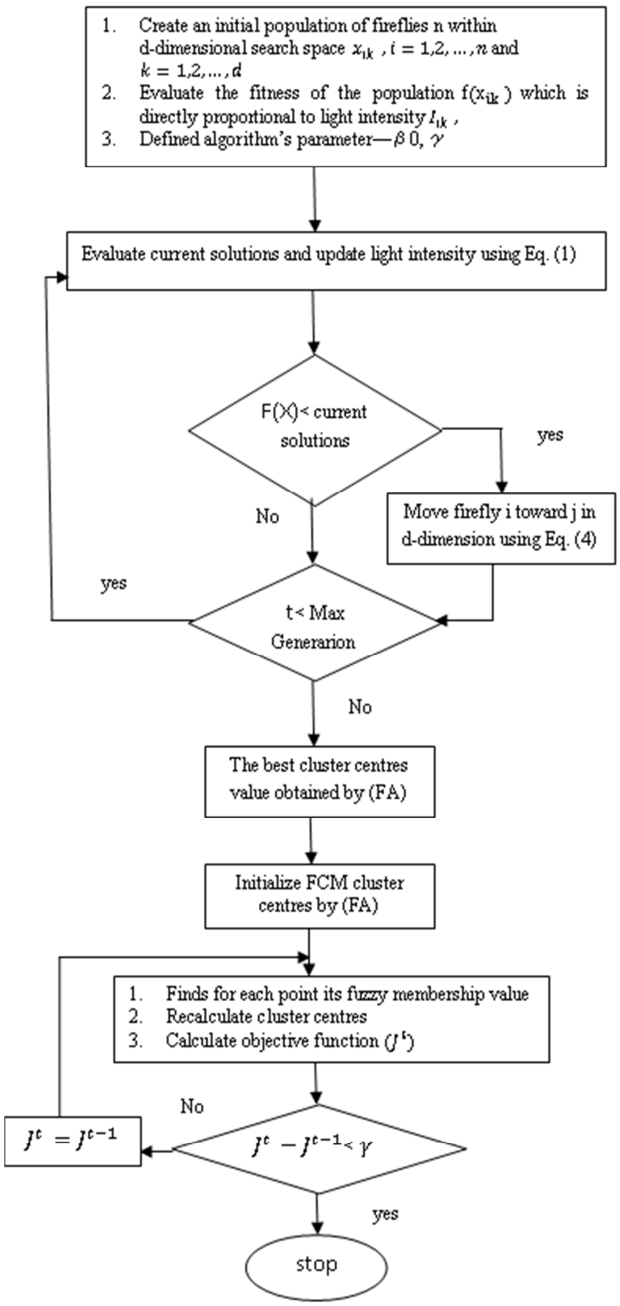

Fig .3. Proposed FFCM Framework.

For the purpose of delineating the connection between the clustering and image segmentation, we claim that it is possible to map every single pixel in an image as a sample or data point in the clustering sector, while it is also possible to map the image regions as clusters or classes. In the case of a 256 x 256 image, there will be 65,536 pixels (data points). For instance, in a given grey image with three distinct regions (e.g., the white matter (WM), grey matter (GM) and cerebrospinal fluid (CSF) in a MRI image of the brain), 8-bit depth, and three features (e.g., intensity value, entropy, and energy), which illustrate each and every pixel, the probable degree of pixel intensity value pertaining to the depth of image will be in the interval $\in[0,255]$, and the deterioration and energy features can be illustrated by interval $\in [0,10]$. Therefore, the firefly solution could be (5, 2.5, 2.6, 30, 6.2, 2.1, 80, 2.3, 1.3), in which the first three digits (5, 2.5, 2.6) signify the cluster centre values for the first image region in each image sequence, and the next three digits (30, 6.2, 2.1) indicate the cluster centre values for the second image region, while the final cluster centre (80, 2.3, 1.3) indicates the third image spot. Immediately after the firefly sets the factors ((n) number of fireflies, β, γ, max generation), the initialization step of the firefly search is examined. All the cluster centres in all the solutions might be randomly initialized from the data range of their image attributes.

Then the fitness value is measured for all the solutions by the objective function and later, the solutions are reorganized in descending order of the objective function value. After choosing the minimal values by comparing the solutions with the objective function, the FA finds near-optimal cluster centres that guarantee that fuzzy c-means will reach near-global optima and will not be trapped in a local optima. This leads to an improvement on the FCM and thus FFCM can replace the traditional method of multiple random initializations to determine cluster centres.

The fitness degree of the solution is indicated by the assessment (fitness value) of each solution. In the present study we used an enhanced version of the conventional FCM objective function[24], because the cluster centres are just employed in the evolving process of the first stage of the FFCM. The enhanced FCM objective function depends merely on the calculations of the cluster centres, whereas the membership matrix U, as in the standard objective function, is not employed, and paid out for the required changes. According to Hathaway and Bezdek (1995), generally, standard and reformulated objective functions are comparative; however, the latter is less complicated. Consequently, the time consumed in determining the objective function for each solution is minimized. The reformulated version of the FCM's objective function is as follows:

ISSN: 1992-8645 www.jatit.org E-ISSN: 1817-3195

$$R_m = \sum_{i=1}^{n}\left(\sum_{j=1}^{c} D_{ji}^{\frac{1}{1-m}}\right)^{1-m} , \quad (11)$$

where D_{ij} is $\|x_i - v_j\|$ the distance from pixel intensity x_i to the jth cluster centre, m is the fuzziness of the resulting classification and it is set $m = 2$ and n is the total number of pixels in the given image. In this case, we measured the aggregate of the distances between all the pixels in the given image with each cluster centre that was produced from the new solution. However, the FA will attempt to reduce this value of R_m (cluster validity) to find the preferred near-optimal solution or to fulfil the stopping criterion.

The objective function is computed for each new firefly solution f(a′),for the purpose of updating the solutions with the newly generated, $a' = (a'_1, a'_2, a'_3, \dots, a'_N)$, if the value of objective function of the new solution is superior to theworst solution stored, then the latter is replaced by the new solution or else this new solution is disregarded.

The iteration process of the evolving procedures of the FA will be ended after achieving the optimum number of improvisations (max generations). Ultimately, the ideal solution is chosen and is regarded as the finest solution to the examined problem. However, such clustering methods consume a huge amount of time, especially in the case of a large number of objects [25].Therefore, it is essential to include a simplification phase to enhance the efficiency of the firefly search by minimizing the number of objects to be clustered, which in turn will minimize the time needed to find the near-optimal solution. The simplification process depends on obtaining the rate of incidence of each pixel in the examined image (like a histogram). Consequently, the image is depicted in a model such as $X = \big((x_1, h_1), \dots, (x_i, h_i), \dots, (x_q, h_q)\big)$, where h_i is the rate of incidence x_i in the image and q is the total number of distinct x values in the image with $(\sum_{i=1}^{q} h_i = n)$. Therefore, the objective unction can be reformulated as follows:

$$R_m = \sum_{i=1}^{n} h_i \left(\sum_{j=1}^{c} D_{ji}^{\frac{1}{1-m}}\right)^{1-m} \quad (12)$$

FCM-based clustering

The FCM algorithm starts with the cluster centers obtained from the FA as initial cluster centers at every iteration and it determines the fuzzy membership of each data point in relation to every cluster by Eq. 7. Based on the membership values, the cluster centers are recomputed by Eq. 8. The FCM stops when there is no further change in the cluster centers.

4. EXPERIMENTS AND RESULTS

This section explains the evaluation of the proposed solution (FFCM) and compares the outcomes with those of several previous methods and the results acquired from the conventional FCM clustering algorithm, namely the random initialization technique of FCM. This section is divided into six parts. The first part describes the data set. The second part analyses the FFCM parameters and the best parameter values are selected. In the third part, the cluster validity (Rm) index is introduced as a quality measurement. In the fourth part, the FFCM is applied to a simulated brain MRIdata set. In the fifth part, the FFCM is applied to a real brain MRI data set. In the final part, the execution times of FFCM for both types of image representation are presented.

4.1 Data set

The data set comprises two different groups of 3D MRI images for the purpose of illustrating the efficacy of the proposed FFCM algorithm. The first group comprises seven normal images and ten abnormal simulated T1-weighted MRI brain images (T1WI), which were acquired from the simulated brain data set of McGill University [26].The size of all these images is 217 × 181 with 8-bit greyscale level. The second group comprises 20 normal 3D MRI real images which were acquired from Internet Brain Segmentation Repository (IBSR), Centre for Morphometric Analysis, Massachusetts General Hospital Repository [27].

4.2 Analysis of firefly parameters

it is crucial to choose appropriate factors for the purpose of accomplishing ideal outcomes from any optimization algorithm, because these factors are vital for the effectiveness and precision of the algorithm. The primary goal of this section is to examine the attributes of the FA during the search process on diverse configurations of four parameters (i.e., number of fireflies (n), β, γ, (T) max generation). Table 1 shows seven test cases

ISSN: 1992-8645 www.jatit.org E-ISSN: 1817-3195

for various configurations to demonstrate the convergence behaviour of the FA. Every single designed case was executed 10 times with the repetition numbers set to 1,000 for all runs. We roughly tested different values for n varying from 1 to 120 and thereby identified that the acceptable value of n is close to 120. Consequently, the n in the majority of the examined cases (see Table 1) was fixed to 120, and every individual case was examined on three MRI real images and six MRI simulated images.

Table 1. Ffcm Convergence Scenarios.

Scenarios	N	γ	β	T
1	1	0.1	0.9	5000
2	20	0.2	0.95	5000
3	40	0.4	0.98	5000
4	60	0.5	0.98	5000
5	80	0.7	0.99	5000
6	100	0.8	0.99	5000
7	120	1	1	5000

Table 2 illustrates the best, mean, worst, and standard deviation of the objective function of every single case. We have highlighted the ideal outcome in bold (i.e., minimum objective function as in Eq. 12) among all cases for every single image. Case S1 (scenario 1, Table 1; S1, Table 2) functions as a local search-based algorithm, which depends on one particular option, s. This case depends on the preliminary arbitrary solution. This inhibits the FA in terms of its ability to examine the search space of the presented image, because α=0.1. Moreover, it is not possible to enhance the solution. This case has weak effectiveness (see Table 2), because it quickly ends in local optima.

Case S2 shows the potential of the FA to boost a novel population of solutions that is dependent on the n of fireflies. This case exhibits the optimistic impact of a greater number of solutions. Case S2 outcomes are completely influenced by preliminary solutions, which are arbitrarily produced and saved. Nevertheless, the efficiency of the second case is superior to that of the first case, despite the fact that identical factors were used for these cases, besides the firefly search. However, they are both significantly less effective than cases S3 and S4 in which the exploration behaviour of the firefly search is enhanced, because the light absorption coefficient is increased to β=0.98, and the potential of exploring unvisited regions of the search space is higher. Consequently, the convergence speed of the firefly γ reached γ=0.5 may be positively affected. In cases S5, S6 and S7, the firefly search utilizes the strength of the light absorption coefficient to pick superior solutions at this point. Similarly, the firefly search is capable of exploring unvisited regions in the given search space through using the light absorption coefficient, where β is 0.99 and 1 correspondingly. These cases are capable of utilizing the advantages of the firefly search to simultaneously check several search space regions while focusing on the most encouraging regions, which consequently results in the most ideal outcomes being achieved by these cases. Based on our analysis, case S7 was chosen to carry out tests in this section, where the firefly variables are set as follows: n=120, β=1, g=1 and the maximum number of iterations (t) is 5,000.

ISSN: 1992-8645 www.jatit.org E-ISSN: 1817-3195

Table 2. Evaluation Of Ffcm Parameters

Image		S1	S2	S3	S4	S5	S6	S7
V 1_24	best	74608332.27	67045531.1	68122927.59	67061418.67	67043656	67043284.52	67043131.21
	mean	97251089.82	100349888.5	105207573.4	78020713.03	68724467	68743098.98	68721503.97
	worst	141942116.3	151122518.7	154443918.3	151124653.6	70158678	70207601.47	70137365.22
	std	29886722.1	35267261.29	41220168.24	25810888.72	883713.55	907998.2403	879803.502
V 8_4	best	74469409.71	75891683.89	74463405.25	74668697.49	74463046	74466932.98	74462757.49
	mean	93550739.51	110672332.6	89815061.48	85878224.45	75009582	79415388.38	79847566.04
	worst	139218734	151841885.4	140803430.6	134832589.1	75880082	119276072.8	123479217
	std	26740960.4	31540217.71	26249625.21	21848051.9	482773.41	14012686.07	15337928.91
V 205_3	best	72470682.75	71525546.26	70786702.97	71661270.44	70426241	70433097.86	70426790.28
	mean	82521782.57	97236705.63	88386399.55	97594489.53	72218850	72260767.82	72218191.74
	worst	100423710.3	142103211.5	141726869.9	141739016.6	73572240	73853466.78	73571244.82
	std	10788499.35	28024901.93	22132364.43	28170378.69	969491.35	1007898.469	971478.3116
Nz1	best	79014182.8	72690595.21	71940397.35	72461113.25	71838019	71836517.5	71836020.06
	mean	96794887.08	83128943	80670145.71	88606125.58	76878311	73012626.02	73062282.04
	worst	119623228.1	111906917.7	103973672	106460447.5	110247542	73976109.38	74063204.39
	std	14697758.31	15103931.67	10981185.01	11616921.13	11756859	622538.6075	698818.2177
Nz36	best	84160248	78894878.85	80642574.28	81008881.09	79829347	78887403.23	78883892.04
	mean	100417857.4	96646749.34	98294727.54	96814317.03	84744637	81407299.96	85047414.17
	worst	124436136.6	113795594.1	117314482.1	115601305.1	116484432	86836016.21	122816896.4
	std	12678813.1	12788298.94	13385719.3	14953166.32	11176814	2142506.168	13308283.05
Nz108	best	9184863.932	83848280.31	84867577.48	83648781.26	83655416	83690801.25	83639954.41
	mean	6502427.275	96111420.76	99312252.65	91539702.64	84515813	84525777.95	84498431.09
	worst	6832663.75	116179658.7	115079363.3	109471687.8	85286048	85269196.24	85283418.94
	std	217335.756	11135468.37	11839223.57	10895407.97	590975.97	569994.7092	608319.0737
Nz144	best	8171719.616	6192189.159	6179515.612	6180112.245	6181642.9	6199314.091	6203719.376
	mean	9830206.973	6435822.958	6382173.696	6531678.678	6555476.1	6416424.667	6416063.205
	worst	14690555.22	6787362.992	6875846.591	6980448.183	7024259.5	6903028.612	6866926.631
	std	2376300.082	210420.2592	272142.3322	309587.6903	357144.56	234046.6455	224382.5434
MSLz1	best	8167329.222	8167495.638	8167489.62	8167400.581	8167256.8	8169135.936	8170655.689
	mean	7338037.574	10931944.31	9135220.233	9049564.681	8181407.9	8170964.316	8260892.392
	worst	7627236.571	14670257.27	11862302.73	14884900.8	8275720.1	8174403.545	8967245.466
	std	313774.6939	2714784.431	1483984.152	2146576.766	33368.657	1602.550604	249945.2348
MSLz5	best	6180363.331	6953005.1	6971244.225	6953262.292	6953346.3	6968898.994	6153372.214
	mean	6645960.597	7393654.323	7270117.003	7160794.485	7395112.2	7181008.137	7178972.921
	worst	7072667.637	7608283.617	7693641.55	7566164.503	7579609.6	7565466.894	7561201.947
	std	282200.837	281737.9848	286973.8383	249385.7828	272393.15	263903.7998	271014.4155

ISSN: 1992-8645 www.jatit.org E-ISSN: 1817-3195

Table 3. Comparative Results (Rm) Between Fcm And Fcm.

Image	Method	PC	PE	XB	Rm
V 1_24	FFCM	0.879404	0.237179	0.000799	67043749
	FCM	0.879405	0.237178	0.000799	67430684
V 8_4	FFCM	0.865383	0.264834	0.000803	74696567
	FCM	0.865384	0.264831	0.000803	75974061
V205_3	FFCM	0.867526	0.261788	0.000895	70428267
	FCM	0.867529	0.261783	0.000895	70795134
Nz1	FFCM	0.864492	0.267963	0.00087	71892044
	FCM	0.864511	0.267928	0.00087	87755933
Nz36	FFCM	0.846116	0.302557	0.001052	78888625
	FCM	0.846146	0.3025	0.001052	84434510
Nz108	FFCM	0.84053	0.31214	0.001	83643996
	FCM	0.84055	0.312103	0.001	85667812
Nz144	FFCM	0.778607	0.183036	0.001471	6241319
	FCM	0.777622	0.183663	0.101295	6533914
MSLz1	FFCM	0.897963	0.089005	0.000506	8167285
	FCM	0.89797	0.088998	0.036825	12918686
MSLz5	FFCM	0.862987	0.114635	0.000846	7025565
	FCM	0.841994	0.130859	0.10682	7093692

Table 4. Comparative Results Based On Different Validity Indices And Objective Function.

images	FFCM		FCM	
	AVG Rm	SD±	AVG Rm	SD±
V 1_24	68730248	885809.1	74313563	11301955
V 8_4	74998354	478511.8	85187983	11770134
V 205_3	79030282	21794694	79319368	8836978
Nz1	72996452	619726.8	92058746	25458388
Nz36	83929453	9330378	84778061	5342354
Nz108	87270510	8808884	87843696	3891235
Nz144	6424714	265892	7074611	629600.4
MSLz1	4372070	97024	7030067	8786194
MSLz5	13629834	2257487	26269632	30746101

ISSN: 1992-8645 www.jatit.org E-ISSN: 1817-3195

5.3 Cluster validity index

The excellence of the solution created is assessed with regards to the intent function. The tests are designed to analyse the efficiency of the firefly search in obtaining suitable preliminary cluster centres for the FCM algorithm, as against the conventional random initialization technique employed to select cluster centres. The outcomes for the FCM with firefly search initialization are designated as FFCM, whereas the outcomes for the FCM with random initialization are denoted as FCM. In the present study we employed the intent function value as a measure of the goodness of clustering. We documented the typical and the standard deviation results of FCM and FFCM from 50 trials. All the tests were carried out on an Intel Core5Duo 2.5 GHz machine, with 4GB RAM. The codes were written using Matlab 2010a.

Table 3 illustrates the above mentioned outcomes, where the first column represent images name, the second column signifies the average and standard deviation value for objective function acquired from the search process of the FA in identifying near-optimum cluster centres, and the initial stage of FFCM method. The third columns depict the average objective function and standard deviation value for FCM, respectively.

These outcomes indicate that the majority of the analysed images show considerable enhancements with respect to minimization of objective function values when using the proposed algorithm FFCM as against FCM. The bold items in Table 3 signify equivalent or superior outcomes of FFCM as compared with FCM. In addition, and from a more detailed investigation of these results , it is evident that FFCM is more constant and reliable than FCM with respect to the acquired standard deviation measurements. On the ther hand, some images still failed to display any enhancements. This result encouraged the author to employ another better measurement and examine the effectiveness of using the objective function as a measurement of the superiority of clustering outcomes. Hence, a cluster quality listing was employed as a functionality metric. A cluster quality list is generally applied to gauge the quality of clustering algorithms.

The present study employed three of the most well-known fuzzy cluster validity indices, namely the PC, PE, XB, in addition to the Rm. These indices are primarily employed to gauge the solidity and uniqueness of the clustering results. A decrease in the values of the XB and PE indices is preferred, whereas an increase in the PC index value is viewed as ideal. Hence a reduction or an improvement in these indices discloses the quality of the clustering. The values in Table 4 illustrate the outcomes with respect to utilizing these cluster validity indices as quality measurements. The result of FCM and FFCM applied to each image is shown for each index.

To aid our analysis of the results presented in Table 4, we categorized the images into two groups. The first group of outcomes closely estimated the objective function values between FFCM and FFCM, as in cases 1, 3 and 9. The second group has lower objective function values for FFCM as against FCM, as in cases 2, 4, 5, 6, 7 and 8. The first group is a normal case, where the estimated values of the objective function obtained by FFCM and FCM need to suggest estimate values for the outcomes acquired by cluster validity indices, which is the case that has been obtained. In the second group, the values of the objective function obtained by FFCM are significantly lower than those of FCM. This is superior regarding the objective function, which has been employed and the outcomes acquired by cluster validity indices reveal in the identical course, where the values of cluster validity in FFCM is superior than FCM, which is also the case, which has been acquired. This means that based on the objective function values, the clustering output of FFCM is better than that of FCM. Consequently, the outcomes acquired from our proposed algorithm are superior to those of the FCM algorithm with random initialization across the four quality measurements used here.

5.4 Simulated MRI brain data

In the present study, the experiment was applied to 17 MRI images that were T1-weighted with 3% noise, 1-mm slice thickness and 20% intensity non-uniformity. The volume size of 1 x 1 x 1 mm^3 with voxel and comprise 181 images with size 217 x 181. These images can consist of many different tissue types based on the tissue location in the image. The normal MRI brain images comprise 10 regions of brain tissues, where the regions are dissimilar between the different z planes. These regions are the CSF, GM, background, WM, skin, skull, fat, glial matter, muscle/skin and connective tissue. The abnormal MRI brain images (including multiple sclerosis lesions) comprise 11 regions; all those seen in the normal images and in addition the multiple sclerosis lesion region. Some of

ISSN: 1992-8645 www.jatit.org E-ISSN: 1817-3195

regions' tissues have the same intensity in the MRI images such as the WM and connective tissues, skull and background, skin and CSF. Therefore, in the present study after merging those regions having the same level of intensity and removing the skull, the clusters numbered six in the normal images and seven in the abnormal images.

The Brain Web [26] provided the ground truth images, and a quantization index was used to evaluate segmentation performance, based on the segmentation accuracy. The accuracy rate was computed based on the similarity between the ground truth image and the segmented images generated by FFCM and FCM. The Minkowski Score (MS) is the quantization index used in the present study [28], which is computed as follows:

$$MS(T,S) = \sqrt{\frac{n_{01}+n_{10}}{n_{11}+n_{10}}}\ , \qquad 13$$

Fig. 4a. From Left To Right, Original Normal MRI T1 Image In Z1, Ground Truth Normal MRI T1 Image In Z1, And Normal MRI T1 Image In Z1 Segmented By FFCM.

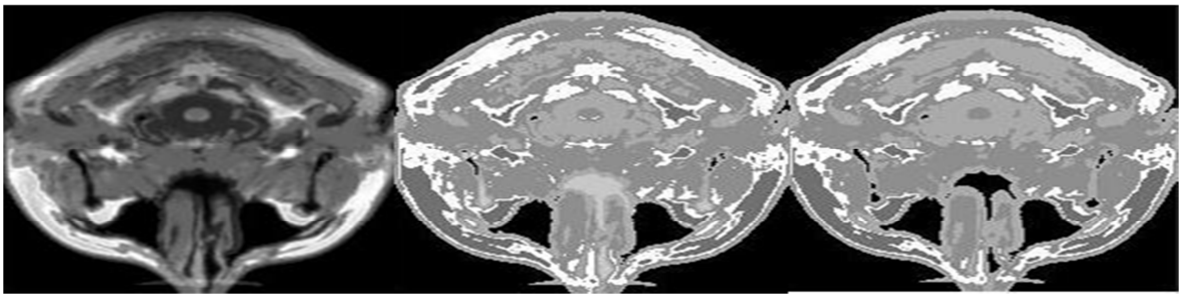

Fig. 4b. From Left To Right, Original Normal MRI T1 Image In Z36, Ground Truth Normal MRI T1 Image In Z36, And Normal MRI T1 Image In Z36 Segmented By FFCM.

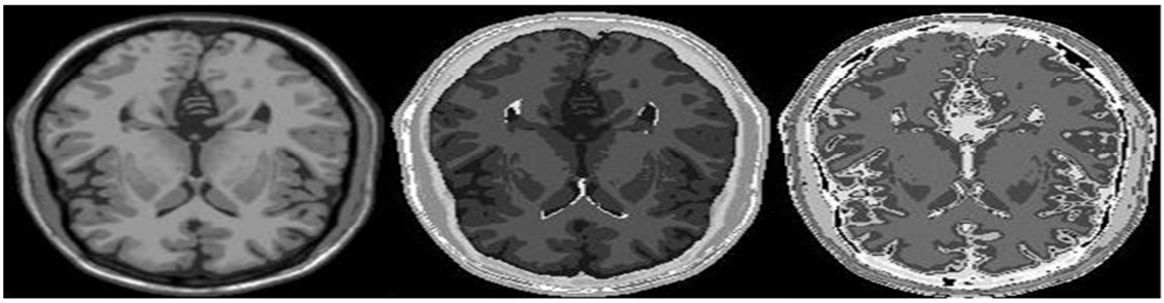

Fig. 4c. From Left To Right, Original Normal MRI T1 Image In Z72, Ground Truth Normal MRI T1 Image In Z72, And Normal MRI T1 Image In Z72 Segmented By FFCM.

Journal of Theoretical and Applied Information Technology
10th March 2014. Vol. 61 No.1

ISSN: 1992-8645 www.jatit.org E-ISSN: 1817-3195

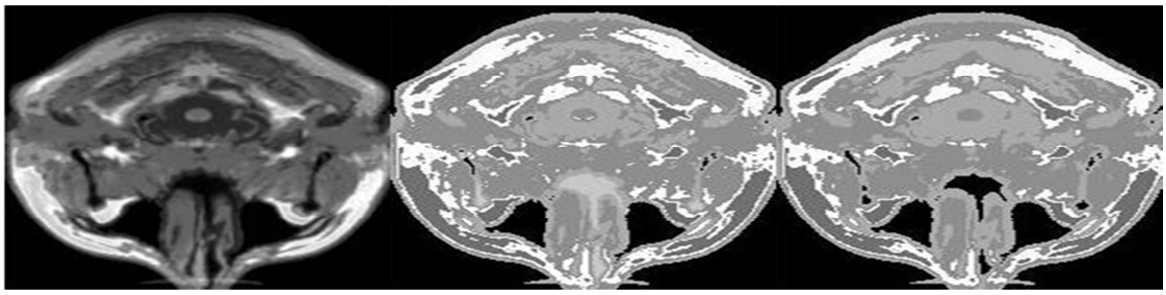

Fig. 5a. from left to right, original multiple sclerosis lesions in MRI T1 image in z1, ground truth multiple sclerosis lesions in MRI T1 image in z1, and multiple sclerosis lesions MRI T1 image in z1 segmented by FFCM.

Fig 5b. from left to right, original multiple sclerosis lesions in MRI T1 image in z5, ground truth multiple sclerosis lesions in MRI T1 image in z5, and multiple sclerosis lesions in MRI T1 image in z5 segmented by FFCM.

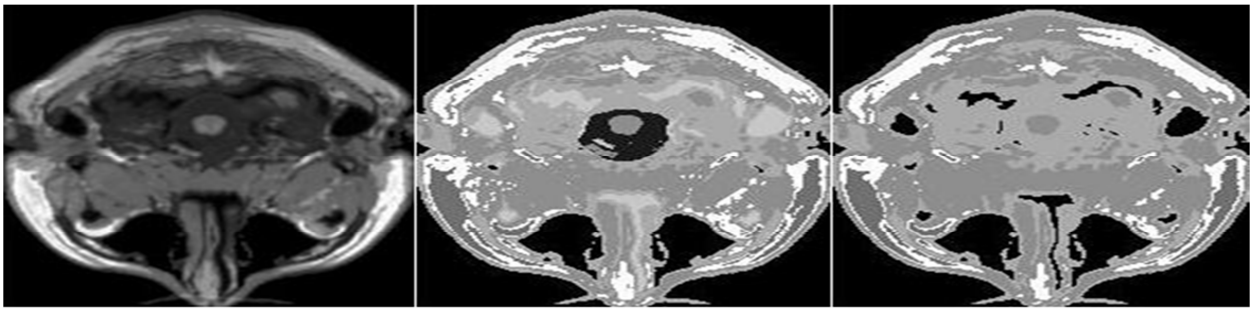

Fig. 5c. from left to right, original multiple sclerosis lesions in MRI T1 image in z10, ground truth multiple sclerosis lesions in MRI T1 image in z10, and multiple sclerosis lesions in MRI T1 image in z10 segmented by FFCM.

TABLE 6. Comparative results: Minkowski Score (MS) for abnormal brain images showing multiple sclerosis lesions.

Z plane	MS (FFCM)	MS (FCM)	MS(EM)
1	0.39	0.64	1.21
2	0.38	0.64	0.80
3	0.78	0.76	0.74
4	0.33	0.73	0.79
5	0.32	0.65	0.69
6	0.32	0.78	0.85
7	0.35	0.76	0.74
8	0.36	0.78	0.79
9	0.38	0.73	0.76
10	0.49	0.69	0.70

ISSN: 1992-8645 www.jatit.org E-ISSN: 1817-3195

where T represents the ground truth image and S represents the segmented image. n_{11} represents the number of pairs of elements that are in the same region in both T and S, while n_{10} represents the number of pairs in the same region in T and n_{01} represents the number of pairs in the same region only in S. The best similarity between the ground truth image (T) and the segmented image (S) is the minimum value of the MS, where the best value for MS equals 0.

In the first experiment (normal simulated MRI brain images), the MS accuracy rate obtained by FFCM showed very good segmentation outcomes. Table 5 shows that the MS accuracy rate obtained by FFCM was much better than that by FCM for five segmented images (z1, z2, z3, z36, z108) and MS accuracy rate obtained by FFCM was much better than that by Expectation Maximization (EM) for five segmented images (z1, z2, z3, z36, z144). While The MS for FCM is better than FFCM for two segmented images (z72, z144) and the MS for EM is better than FFCM for two segmented images (z72, z108) because the ground truth images have a different number of clusters, and thus the matching MS test was affected. Figure 4 shows, from left to right respectively, the original image, ground truth image and image segmented by FFCM.

In the second experiment (abnormal simulated MRI brain images), the MS accuracy rate obtained by FFCM produced excellent segmentation outcomes. Table 6 shows that the MS accuracy rate obtained by FFCM was much better than that by FCM and EM for nine segmented images (z1, z2, z4, z5, z6, z7, z8, z9, z10), while the rest were comparable. The MS for FCM and EM was better than for FFCM for one segmented image (z3) because the ground truth images have a different number of clusters, and thus the matching test (the MS) was affected. Figure 5 shows, from left to right respectively, the original image, ground truth image and image segmented by FFCM.

TABLE 5: Comparative Results: Minkowski Score (MS) For Normal Simulated Images.

Z plane	MS (FFCM)	MS (FCM)	MS(EM)
1	0.39	0.7	1.019
2	0.38	0.65	0.83
3	0.36	0.62	0.64
36	0.87	0.88	1.12
72	0.78	0.72	0.70
108	0.61	0.79	0.58
144	0.69	0.34	0.76

5.5 Real MRI brain data

In the present study, experiments were also conducted to apply the FFCM to real 3D MRI brain images downloaded from the IBSR [27]. This set comprised 20 normal MRI brain images with ground truth images manually segmented by experts. These images are T1-weighted with a resolution of 256 x 256 x 64, and the size of voxel is 1.17 x 1.17 x 3.1 mm^3, downloaded from many 1.5-Tesla GE/Siemens MRI scanners. The reasons for choosing this type of images is the difficulty encountered in segmentation due to variations in shape complexity, low signal to noise ratio and severe spatial intensity non-uniformity [29]. The first step in this experiment was to remove the undesirable tissues such as bone, fat and skull from the original and from the ground truth images to arrive at the region of interest. Figure 6 illustrates this process.

The accuracy rate was computed based on the similarity between the ground truth image and a segmented image by FFCM. The Tanimoto coefficient T $\in$ [0,1] [30] was the quantization index used in this part of the study. The Tanimoto coefficient T is used as an overlap metric and is reported on the IBSR website. It is computed as follows:

$$T = \frac{|A \cap B|}{|A \cup B|} \quad , \qquad 14$$

where A represents the number of voxels in the ground truth and B represents the number of voxels in the FFCM segmented image. The best similarity between A and B is the maximum value of T, and the best value for T equals 1. Figure 7 shows, from left to right respectively, the original image, ground truth image and image segmented by FFCM.

The T for FFCM is shown in Figs. 8, 9 and 10 in comparison with the outcomes from six different segmentation methods on the IBSR website, namely Adaptive MAP (AMAP), tree-structure k-means (TSK), maximum a posteriori probability (MAP), FCM, Bias MAP (BMAP), and maximum-likelihood (MLC). Furthermore, Table 7 shows the T for FFCM in comparison with the outcomes of the above six methods and four additional published state-of-the-art methods [7], namely the adaptive mean shift algorithm (AMS), the MPM-MAP algorithm, constant-bandwidth mean shift algorithm (fixedwMS), and adaptive field rule (AFR).

ISSN: 1992-8645 www.jatit.org E-ISSN: 1817-3195

From Figs. 8, 9 and 10 and Table 7, it can be seen that the FFCM outcomes are much better than those produced by all the other algorithms in the case of the WM tissue segmentations. Moreover, FFCM is also better than the algorithms from the IBSR website in the case of the GM tissue segmentations, but it is not better than two state-of-the-art methods (MPM-MAP, AMS). For CSF tissue, the FFCM results are better than all algorithms except for one of the state-of-the-art methods, (Fixed wMS). Finally, the FFCM outcomes for WM tissues segmentation are better than those for CSF and GM tissue segmentation. This is due to MRI images artifacts and the intensity levels similarity between CSF and GM.

5.6 FFCM execution time

The execution time to segment MRI images (simulated and real) by FFCM took more than one hour; however, the simplified process for the objective function described in Section 4.1 reduces the execution time for the segmentation of MRI images (simulated and real) by FFCM to around 4 s. Thus, this process minimizes the execution time and makes the FFCM algorithm more efficient.

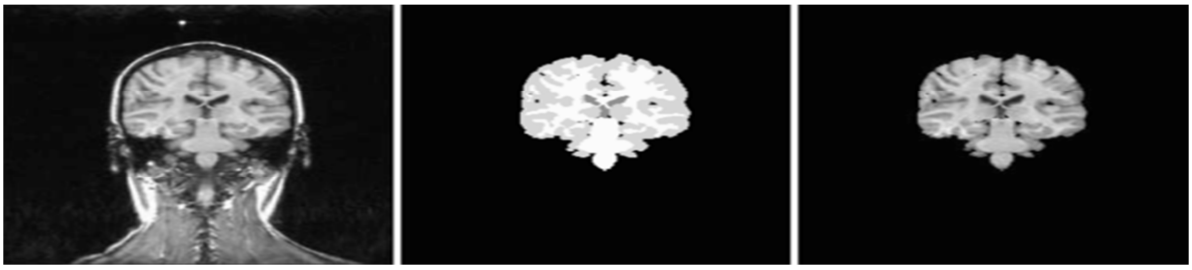

Fig 6. Tissue removal steps from left to right, original volume 16_3 (slice #22), ground truth, region of interest.

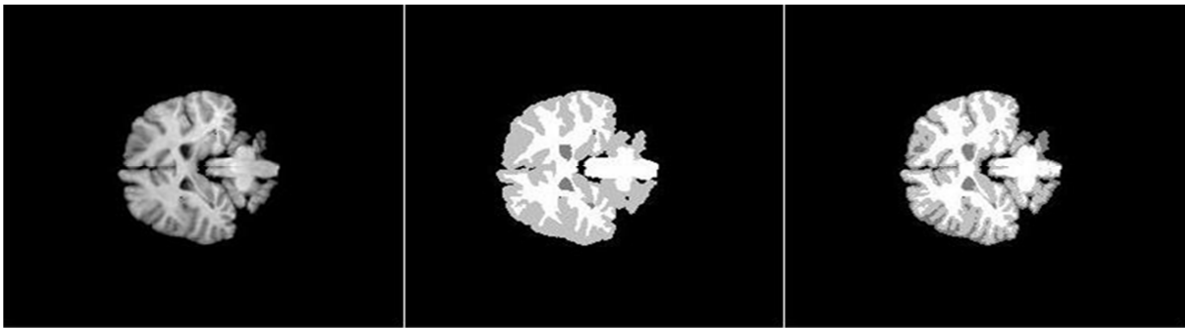

Fig 7a. From Left To Right, Original Volume (1_24), Ground Truth Volume (1_24), And Segmented Volume (1_24) By FFCM.

Journal of Theoretical and Applied Information Technology
10th March 2014. Vol. 61 No.1

ISSN: 1992-8645 www.jatit.org E-ISSN: 1817-3195

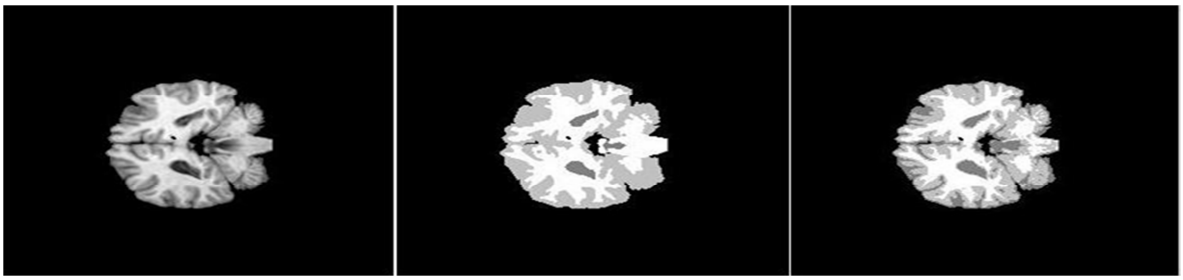

Fig 7b. From Left To Right, Original Volume (8_4), Ground Truth Volume (8_4), And Segmented Volume (8_4) By FFCM.

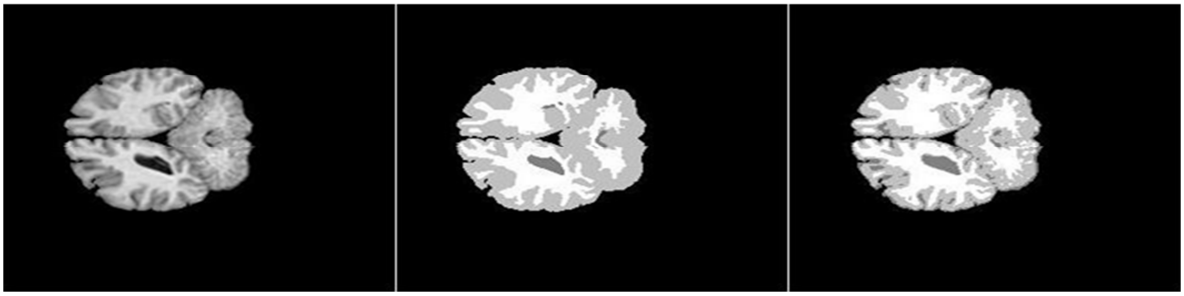

Fig 7c .From Left To Right, Original Volume (205_3), Ground Truth Volume (205_3), And Segmented Volume (205_3) By FFCM.

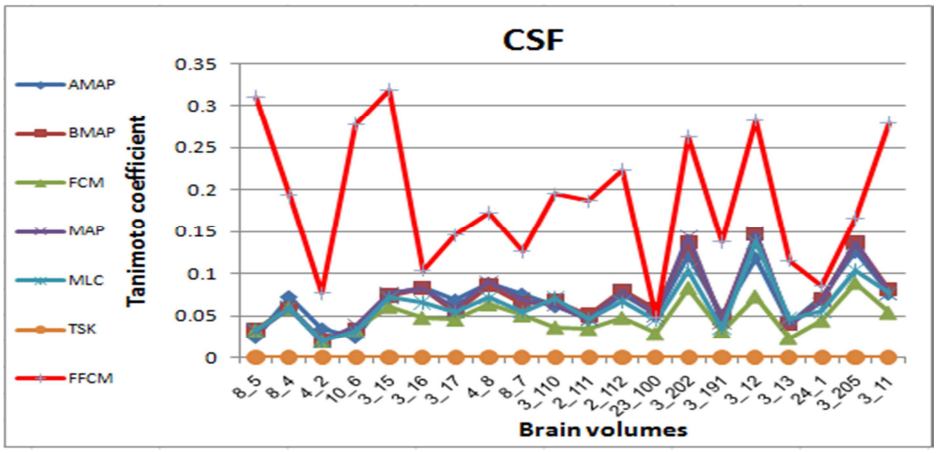

Fig .8. FFCM Tanimoto Coefficient (T) For The 20 IBSR Images Compared With Other Algorithms For CSF.

Journal of Theoretical and Applied Information Technology
10th March 2014. Vol. 61 No.1

ISSN: 1992-8645 www.jatit.org E-ISSN: 1817-3195

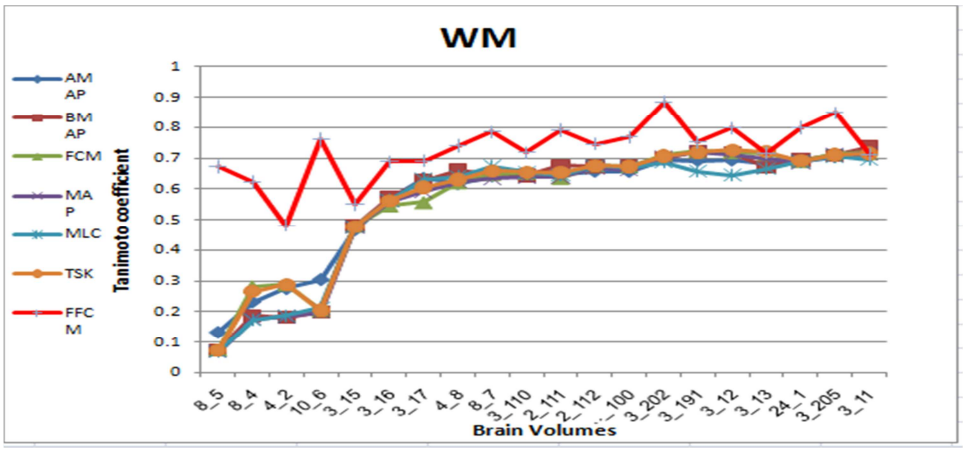

Fig. 9. FFCM Tanimoto Coefficient (T) For The 20 IBSR Images Compared With Other Algorithms For WM.

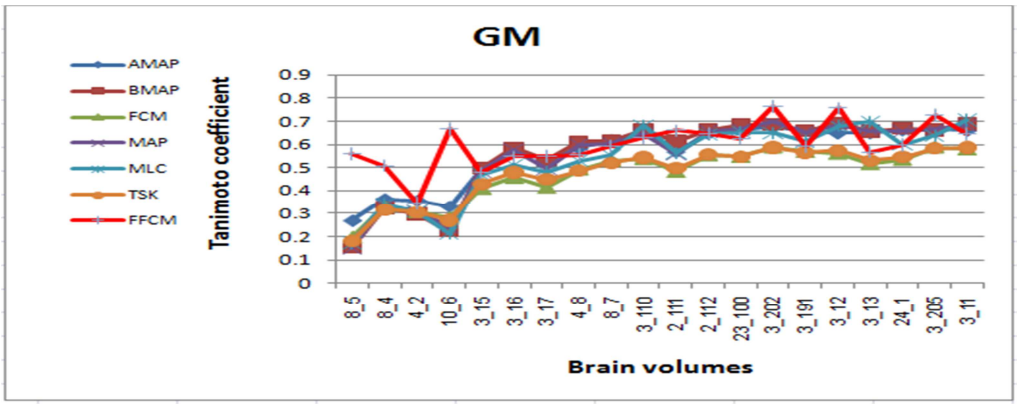

Fig 10. FFCM Tanimoto Coefficient (T) For The 20 IBSR Images Compared With Other Algorithms For GM.

Table 7. Tanimoto Coefficient (T) Outcome Averages For FFCM Segmentation And Other Methods.

Method	CSF	GM	WM
Adaptive MAP	0.069	0.564	0.567
Biased MAP	0.071	0.558	0.562
FCM	0.048	0.473	0.567
MAP	0.071	0.55	0.554
MLC	0.062	0.535	0.551
TSK means	0.049	0.477	0.571
AFR	0.092	0.557	0.587
Fixed wMS	0.21	0.594	0.628
MPM-MAP	N/A	0.662	0.683
AMS	N/A	0.683	0.691
FFCM	0.186	0.600	0.727

6. CONCLUSION

This research proposed a new clustering approach based on the hybridization of firefly algorithm (FA) and fuzzy c-means algorithm(FCM) called (FFCM) to segment MRI brain images. this approach consists of two stages. In the first stage, use the capability of firefly search to find optimal initial cluster centres, then in the second stage, the output of the first stage is used to initialize the FCM, where the later, it performs the clustering process. The proposed algorithm (FFCM) was

ISSN: 1992-8645 www.jatit.org E-ISSN: 1817-3195

employed as an MRI image segmentation method and the outcomes of the segmentation of simulated and real MRI brain images indicated the efficiency of the proposed algorithm in comparison with state-of-the-art segmentation algorithms and the randomly initialized FCM segmentation

ACKNOWLEDGEMENT

This research is based on two research grants from Ministry of Science, Technology and Innovation, Malaysia entitled “Sciencefund 01-01-02-SF0694 Spiking-LVQ Network For Brain Tumor Detection” and Arus Perdana Fund AP-2012-019 entitled “Automated Medical Imaging Diagnostic Based on Four Critical Diseases: Brain, Breast, Prostate and Lung Cancer” . We have obtained Ethics approval entitled “FF-342-2012 Imaging Processing of the Brain Tumor Using LVQ Classifier” from PPUKM or UKM Medical Canter, Malaysia for collecting and conducting experiments on MRI Brain Tumor patient’s record.

REFERENCES

[1] J. A. Richards, Remote sensing digital image analysis: an introduction: Springer, 2013.
[2] M. A. Balafar, et al., "Review of brain MRI image segmentation methods," Artificial Intelligence Review, vol. 33, pp. 261-274, 2010.
[3] D. L. Pham, et al., "Current methods in medical image segmentation 1," Annual review of biomedical engineering, vol. 2, pp. 315-337, 2000.
[4] J. C. Bezdek, Pattern Recognition with Fuzzy Objective Function Algorithms: Kluwer Academic Publishers, 1981.
[5] J. Kang, et al., "Novel modified fuzzy c-means algorithm with applications," Digital Signal Processing, vol. 19, pp. 309-319, 2009.
[6] P. Hore, et al., "A scalable framework for segmenting magnetic resonance images," Journal of signal processing systems, vol. 54, pp. 183-203, 2009.
[7] O. d. Alia, et al., "A hybrid harmony search algorithm for MRI brain segmentation," Evolutionary Intelligence, vol. 4, pp. 31-49, 2011/03/01 2011.
[8] A. Abraham, et al., "Swarm Intelligence Algorithms for Data Clustering," in Soft Computing for Knowledge Discovery and Data Mining, O. Maimon and L. Rokach, Eds., ed: Springer US, 2008, pp. 279-313.
[9] D. Karaboga, et al., "A comprehensive survey: artificial bee colony (ABC) algorithm and applications," Artificial Intelligence Review, pp. 1-37, 2012/03/01 2012.
[10] G. Ingram and T. Zhang, "Overview of Applications and Developments in the Harmony Search Algorithm," in Music-Inspired Harmony Search Algorithm. vol. 191, Z. Geem, Ed., ed: Springer Berlin Heidelberg, 2009, pp. 15-37.
[11] P. M. Kanade and L. O. Hall, "Fuzzy Ants and Clustering," Systems, Man and Cybernetics, Part A: Systems and Humans, IEEE Transactions on, vol. 37, pp. 758-769, 2007.
[12] S. Z. Selim and K. Alsultan, "A simulated annealing algorithm for the clustering problem," Pattern Recognition, vol. 24, pp. 1003-1008, 1991.
[13] R. H. Sheikh, et al., "Genetic Algorithm Based Clustering: A Survey," in Emerging Trends in Engineering and Technology, 2008. ICETET '08. First International Conference on, 2008, pp. 314-319.
[14] L. O. Hall, et al., "Clustering with a genetically optimized approach," Evolutionary Computation, IEEE Transactions on, vol. 3, pp. 103-112, 1999.
[15] K. S. Al-Sultan and C. A. Fedjki, "A tabu search-based algorithm for the fuzzy clustering problem," Pattern Recognition, vol. 30, pp. 2023-2030, 1997.
[16] T. Hassanzadeh and M. R. Meybodi, "A new hybrid approach for data clustering using firefly algorithm and K-means," in Artificial Intelligence and Signal Processing (AISP), 2012 16th CSI International Symposium on, 2012, pp. 007-011.
[17] L. Lili, et al., "A Novel Fuzzy Clustering Based on Particle Swarm Optimization," in Information Technologies and Applications in Education, 2007. ISITAE '07. First IEEE International Symposium on, 2007, pp. 88-90.
[18] X.-S. Yang, "Firefly algorithm, stochastic test functions and design optimisation," International Journal of Bio-Inspired Computation, vol. 2, pp. 78-84, 2010.
[19] J. Senthilnath, et al., "Clustering using firefly algorithm: Performance study," Swarm and Evolutionary Computation, vol. 1, pp. 164-171, 2011.

ISSN: 1992-8645 www.jatit.org E-ISSN: 1817-3195

[20] D. Karaboga and C. Ozturk, "A novel clustering approach: Artificial Bee Colony (ABC) algorithm," Applied Soft Computing, vol. 11, pp. 652-657, 2011.
[21] X.-S. Yang, Nature-Inspired Metaheuristic Algorithms: Luniver Press, 2008.
[22] A. K. Jain, et al., "Data clustering: a review," ACM Comput. Surv., vol. 31, pp. 264-323, 1999.
[23] Q. W. Bsoul and M. Mohd, "Effect of ISRI stemming on similarity measure for arabic document clustering," presented at the Proceedings of the 7th Asia conference on Information Retrieval Technology, Dubai, United Arab Emirates, 2011.
[24] R. J. Hathaway and J. C. Bezdek, "Optimization of clustering criteria by reformulation," Fuzzy Systems, IEEE Transactions on, vol. 3, pp. 241-245, 1995.
[25] J. C. Bezdek, et al., Fuzzy Models and Algorithms for Pattern Recognition and Image Processing: Springer Science+Business Media, Incorporated, 2005.
[26] BainWeb. (Nov 2003, simulated brain database Mcconnell Brain Imaging Centre Montreal Neurological Institute Mcgill University. Available: http://www.bic.mni.mcgill.ca/brainweb
[27] IBSR. (Sep 2005, : internet brain segmentation repository. Technical report, Massachusetts General Hospital, Center for Morphometric Analysis. Available: http://neuro-www.mgh.harvard.edu/cma/ibsr/
[28] A. Ben-Hur and I. Guyon, "Detecting stable clusters using principal component analysis," in Functional Genomics, ed: Springer, 2003, pp. 159-182.
[29] Z. Peng, "Segmentation of white matter, gray matter, and CSF from MR brain images and extraction of vertebrae from MR spinal images," University of Cincinnati, 2006.
[30] R. O. Duda, et al., Pattern classification: John Wiley & Sons, 2012.